

## An Alternative Gaussian Window Approach for FIR Filter Design

Sandip Sarkar<sup>1,\*</sup>, Subhajit Karmakar<sup>2</sup>, Kuntal Ghosh<sup>3</sup> and Swapan Sen<sup>4</sup>

<sup>1,2,4</sup>Microelectronics Division, Saha Institute of Nuclear Physics, 1/AF Bidhannagar, Kolkata-700064, India

<sup>2</sup>Center for Soft Computing Research, Indian Statistical Institute, 203 B. T. Road, Kol-108, INDIA

<sup>1</sup>[sandip.sarkar@saha.ac.in](mailto:sandip.sarkar@saha.ac.in), <sup>2</sup>[subhajit.karmakar@saha.ac.in](mailto:subhajit.karmakar@saha.ac.in), <sup>3</sup>[kuntal\\_v@isical.ac.in](mailto:kuntal_v@isical.ac.in), <sup>4</sup>[swapan.sen@saha.ac.in](mailto:swapan.sen@saha.ac.in)

**Abstract**— The problem of conventional window based FIR filter design lies in its very limited design flexibility and more specifically the lack of control over band edges. We propose an alternative Gaussian window approach for FIR filter design that overcomes these problems of conventional window method. We show that sum of mean shifted Gaussians can be used for flexible filter design. We also derive relations to compute the corresponding impulse response effectively in a non-recursive manner. These relations give precise control over band-edge frequencies. Comparison of precision in control and computational time with other methods is also presented.

**Index Terms**—FIR digital filter, Gaussian window, window method.

### I. INTRODUCTION

The basic idea of conventional window based approach to FIR filter design is to choose an appropriate ideal frequency selective filter that always has a noncausal infinite impulse response. The next step is to obtain a causal, linear phase, finite impulse response (FIR) filter by truncating the ideal impulse response with an appropriate window function [1]. The choice of an ideal filter and a proper window function is therefore very important in this design approach. The most commonly used windows are Rectangular window, Hanning window, Hamming window, Blackman window and the Kaiser window. The major disadvantage of these methods is the lack of design flexibility [2-4]. Band edge frequencies cannot be specified precisely due to the smearing effect of windowing. We propose an alternative method where the filter is constructed by adding mean-shifted Gaussians with same standard deviation. The number of required Gaussians and the standard deviation is a function of filter design parameters. We have derived relations to compute non-recursive the impulse response and also demonstrated the precise control over band edge frequencies and ripple magnitudes. A similar methodology with Gaussian derivatives has been reported in [5], where the solutions were achieved in a recursive manner.

### II. THEORWTICAL FOUNDATION

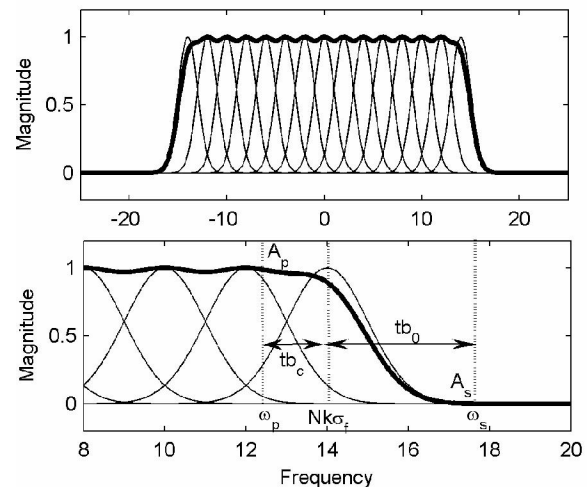


**Fig.1** Basic principle of filter design by adding mean shifted Gaussians. The graphs are drawn with arbitrary units of frequency. The magnitudes are normalized for the sake of illustration. The top figure shows the effect of summation of Gaussians and the bottom one is the zoomed version of the top figure depicting various parameters described in Equation (3). The thicker curve is the Consider the sum of mean shifted Gaussians  $G(\omega, \sigma, a)$  shown in Fig. 1 for the specific case of low-pass (LP) filter design. For the sum of  $2N + 1$  Gaussians

$$\sum_{n=-N}^N G(\omega, \sigma_f, a) = \sum_{n=-N}^N \exp\left(-\frac{(\omega - a)^2}{2\sigma_f^2}\right) \quad (1)$$

$$\text{with the mean defined as } a = nk\sigma_f \quad (2)$$

$N$  depends on the bandwidth  $\omega_p$ ,  $k$  is a suitable constant (usually  $\leq 1$ ) to be defined later and  $\sigma_f$  is the standard deviation. Each Gaussian is therefore shifted by an amount  $k\sigma_f$  from its nearest neighbour. From Fig. 1 we can write the transition bandwidth ( $tb$ ) as:

$$tb = tb_0 + tb_c = \omega_s - \omega_p$$

$$\text{Here, } tb_0 = \omega_s - Nk\sigma_f = k_s\sigma_f - NK\sigma_f \quad (3)$$

$$tb_c = Nk\sigma_f - \omega_p = NK\sigma_f - k_p\sigma_f$$

where  $tb_0$  is the approximate estimate of the transition band width measured from the mean position of the furthest

Gaussian,  $tb_c$  is the correction term for the transition band width,  $\omega_p$  and  $\omega_s$  are the passband and stopband edge frequencies respectively.

The real part of Gaussian and its Fourier transform pair is related by [6]:

$$\sqrt{\frac{\sigma^2}{2\pi}} \cos(xa) \exp\left(-\frac{1}{2}\sigma^2 x^2\right) \leftrightarrow \exp\left(-\frac{(\omega-a)^2}{2\sigma^2}\right) \quad (4)$$

Using the above expression, the impulse response of the filter represented by equation (1) can be written as

$$\begin{aligned} h(x) &= \sum_{n=-N}^N \sqrt{\frac{\sigma_f^2}{2\pi}} \cos(nk\sigma_f) \exp\left(-\frac{1}{2}\sigma_f^2 x^2\right) \\ &= \sqrt{\frac{\sigma_f^2}{2\pi}} \exp\left(-\frac{1}{2}\sigma_f^2 x^2\right) \left(1 + 2 \frac{\cos\frac{(N+1)xk\sigma_f}{2} \sin\frac{Nkx\sigma_f}{2}}{\sin\frac{xk\sigma_f}{2}}\right) \end{aligned} \quad (5)$$

$$\text{using the relation [7]} \quad \sum_{n=1}^N \cos(nx) = \left(\frac{\cos\frac{(N+1)x}{2} \sin\frac{Nx}{2}}{\sin\frac{x}{2}}\right) \quad (6)$$

From equation (5) we see that the summation of Gaussians as in (1) is equivalent to windowing by Gaussian. This gives a number of advantages compared to the conventional window method of filter design. The major advantage is that the question of smearing of the corner frequencies does not arise in this methodology. We are going to show that this expression gives precise control over the parameters for FIR filter design. These expressions can also be easily extended for bandpass and highpass filters.

First, we discuss the procedure for ripple estimation. Fig. 1 depicts the basic principle of ripple generation due to the superposition of Gaussians. It is evident from the figure that the ripple magnitude depends on the amount of overlap between adjacent Gaussians. The higher the overlap the lower the ripple magnitude and vice versa. By definition the overlap is determined by  $k\sigma_f$ . The lower the value of  $k\sigma_f$  the higher the overlap and consequently lower the ripple magnitude. It is also well known that the peak amplitude of any Gaussian given by (1) is unity and the magnitude at any point  $c\sigma_f$  away from its mean position, where  $c$  is any real number, is independent of the magnitude of  $\sigma_f$ . Therefore  $k$  is the only parameter that determines the ripple magnitude. Simulation shows that for  $k \leq 0.5$  the ripple magnitude in the passband is of the order of  $10^{-15}$  when the computation is done in double precision on a 32 bit Pentium-IV processor and remains nearly the same for lower value of  $k$ . It should also be noted that lower the value of  $k$  higher is the number of Gaussians ( $N$ ) necessary for the construction of a filter. We have therefore assigned a much lower typical value  $k = 0.001$  to increase  $N$ . This will help to reduce the error due to the rounding of  $N$  to its nearest integral value.

Secondly, we explain how to evaluate  $\sigma_f$  and the associated  $N$  from the input specifications. To do this, we try

to relate various control parameters in (1) – (3) to the filter design parameters namely, passband and stopband edge frequencies ( $\omega_p, \omega_s$ ), passband and stopband ripple magnitudes ( $A_p, A_s$ ). All these are input parameters for the filter. Defining normalized  $tb$  as  $tb_n = tb / \sigma_f$  we can write:

$$\begin{aligned} &\text{Where, from equation (3),} \\ tb_n &= tb / \sigma_f = tb_0 / \sigma_f + tb_c / \sigma_f = tb_{0n} + tb_{cn} \\ tb_{0n} &= k_s - NK \\ tb_{0n} &= NK - k_p \end{aligned} \quad (7)$$

i.e.  $tb_{0n}$  and  $tb_{cn}$  are independent of  $\sigma_f$ . We can, therefore, estimate  $tb_0$  and  $tb_c$  numerically for any given  $\sigma_f$  and obtain  $tb_{0n}$  and  $tb_{cn}$  through normalisation. To find an empirical relation between  $tb_n$  and  $A_s$  we first draw plots similar to Fig. 1 with  $k=0.001$  and  $\sigma_f=0.01$ . The value of  $\sigma_f$  was chosen arbitrarily, but is kept small to reduce the rounding-off error of  $N$  as discussed earlier. We estimate  $tb_0$  and  $tb_c$  numerically by searching for appropriate  $\omega_p$  and  $\omega_s$  with magnitudes  $A_p$  and  $A_s$  on the curve in Fig.1 and obtain  $tb_n$  and  $tb_{cn}$  after proper normalization as defined in equation (7). For every given value of  $A_p$ ,  $tb_n$  and  $tb_{cn}$  are estimated numerically for each of the values of  $A_s=50, 100, 150, 200, 250, 300$  dB. We thus get six values of  $tb_n$  corresponding to six values of  $A_s$ . On the contrary we get only one value of  $tb_{cn}$  because for a given  $A_p$ , it remains the same as defined in Fig.1. In the next step we express  $tb_n$  as a fifth order polynomial function of  $A_s$  with the help of least square curve fitting. The fifth order polynomial is chosen because it produced the best fit. This procedure is repeated for all values of  $A_p$  and therefore for each  $A_p$  we obtained a fifth order polynomial expression of  $A_s$  as an estimate of  $tb_n$ . In equation (8) four such estimates of  $tb_n$  and  $tb_{cn}$  are shown for  $A_p = 10^{-1}, 10^{-2}, 10^{-3}$  and  $10^{-8}$  dB. The last expression for  $A_p = 10^{-8}$  dB may not be very useful for practical purposes but have been included to check the accuracy of our algorithm

$$\begin{aligned} A_p &= 10^{-1} \text{ dB}, tb_{cn} = 2.276000000000068, \\ tb_n &= 2.4 \times 10^{-12} \times A_s^5 - 2.64 \times 10^{-9} \times A_s^4 + 1.194 \times 10^{-6} \times A_s^3 \\ &\quad - 0.0002982 \times A_s^2 + 0.059 \times A_s + 2.688. \\ A_p &= 10^{-2} \text{ dB}, tb_{cn} = 3.048000000000068, \\ tb_n &= 2.4 \times 10^{-12} \times A_s^5 - 2.64 \times 10^{-9} \times A_s^4 + 1.194 \times 10^{-6} \times A_s^3 \\ &\quad - 0.0002982 \times A_s^2 + 0.059 \times A_s + 3.44. \end{aligned} \quad (8)$$

$$A_p = 10^{-3} \text{ dB}, tb_{cn} = 3.68200000000068,$$

$$tb_n = 2.36 \times 10^{-12} \times A_s^5 - 2.61 \times 10^{-9} \times A_s^4 + 1.1855 \times 10^{-6} \times A_s^3$$

$$- 0.00029708 \times A_s^2 + 0.058942 \times A_s + 4.0755.$$

$$A_p = 10^{-8} \text{ dB}, tb_{cn} = 5.97450000000121,$$

$$tb_n = 2.3333 \times 10^{-12} \times A_s^5 - 2.5783 \times 10^{-9} \times A_s^4 + 1.1725 \times 10^{-6} \times A_s^3$$

$$- 0.00029473 \times A_s^2 + 0.05875 \times A_s + 6.3735.$$

We can now estimate  $\sigma_f$  from (3) as

$$\sigma_f = \frac{\omega_s - \omega_p}{tb_n} \quad (9)$$

and  $N$  can be evaluated from (3) as given by

$$N = \text{round} \left( \frac{tb_{cn} + \omega_p}{k\sigma_f} \right) \quad (10)$$

The last point that we shall discuss now, is how to determine the length of the window. We shall again take the help of numerical procedure to find an empirical relation between the truncation length and the stopband attenuation. The truncation length is expressed in units of standard deviation of the Gaussian as

$$x = \text{round}(m / \sigma_f) \quad (11)$$

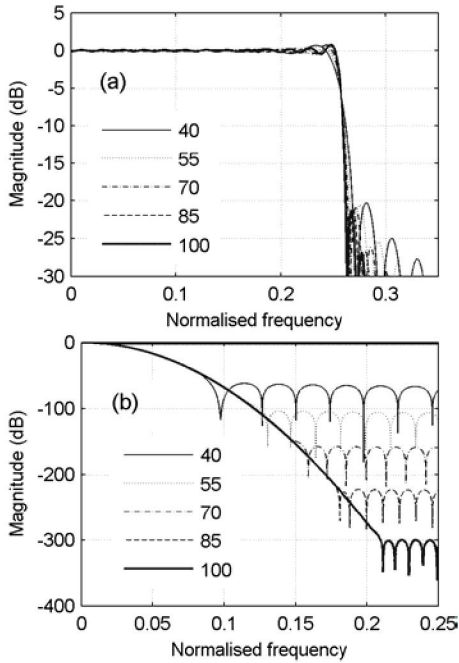


**Fig. 2.** Illustration of the Fourier spectra of (a) of the 2<sup>nd</sup> term in (5) which is a Gaussian and (b) the 3<sup>rd</sup> term in (5) for different truncation lengths. For the sinc like function in (a) the attenuation does not depend on the truncation length whereas for the Gaussian in (b) it is very sensitive to the truncation length. The values with the legends represent the number of taps for various curves.

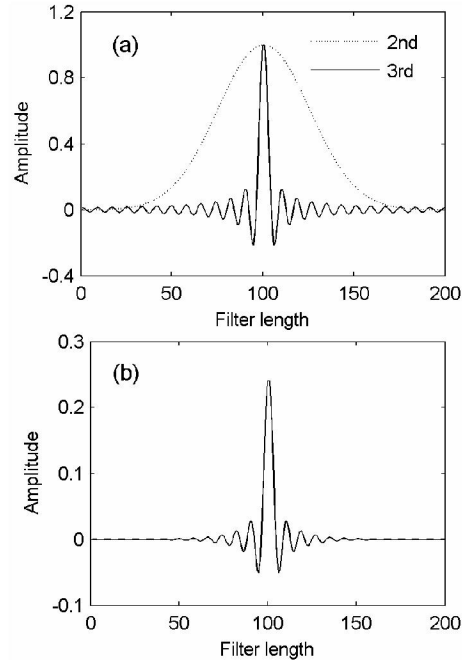


**Fig. 3.** Illustration of windowing operation represented by (5) for a typical filter. In (a) the behaviour of the 2<sup>nd</sup> and the 3<sup>rd</sup> terms in (5) is presented and in (b) the resultant impulse response is shown. Both the curves in (a) are shown in a normalized scale for the sake of illustration.

where  $m$  is a constant to be evaluated. Fourier spectra of the 2<sup>nd</sup> and the 3<sup>rd</sup> term of equation (5) are shown in Fig. 2 for different truncation lengths. The second term is similar in nature to sinc function and therefore the attenuation in the spectrum in Fig. 2(a) does not depend on the truncation length whereas in the spectrum of the Gaussian window in Fig. 2(b), the attenuation is very much sensitive to the truncation length. The resultant attenuation is simply governed by the truncation length of the Gaussian window. To find an empirical relation between  $m$  and  $A_s$  we choose  $A_s = 30, 50, 70, 100, 150, 200, 250$  and  $300$  dB for stopband attenuation keeping other design parameters fixed at some arbitrarily chosen values. Substituting equation (11) in equation (5) the magnitude response of the filter is plotted and  $m$  is manually tuned to fulfill the stopband attenuation requirement given by each  $A_s$  and obtain  $m = 1.1512, 2.2128, 2.8041, 3.7673, 4.9968, 5.9904, 6.8472$  and  $7.6117$  respectively. A fourth order polynomial curve fitting of  $m$  versus  $A_s$  gives the following relation

$$m = -1.135 \times 10^{-9} \times A_s^4 + 9.4594 \times 10^{-7} \times A_s^3 - 3.1119 \times 10^{-4} \times A_s^2$$

$$+ 0.065988 \times A_s - 0.529 \quad (12)$$

This equation is valid for  $30 \leq A_s \leq 300$  dB.

### III. RESULTS

Let us first summarise the steps necessary for filter design. Input parameters for the filter are  $\omega_p, \omega_s, A_p, A_s$  and we need to

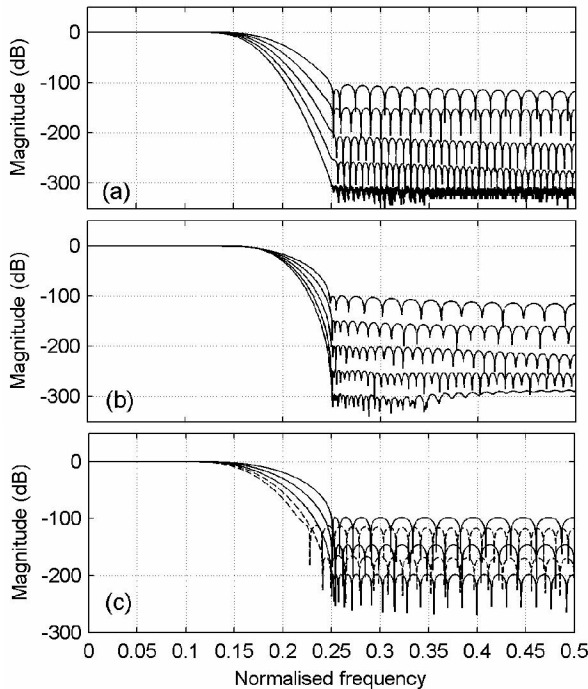


**Fig. 4.** Magnitude response curves of the filters obtained by (a) the proposed Gaussian window method, (b) Kaiser window method and (c) optimal method (Parks-McClellan algorithm) are shown for stopband attenuations 100, 150, 200, 250 and 300dB. The passband edge was  $f_p = 0.1$  and the stopband edge was  $f_s = 0.25$  for all the cases.

evaluate the required impulse response  $h(x)$  from (5) for which we need to know  $\sigma_f$ ,  $N$  and  $x$ . First we have to evaluate  $\sigma_f$  from (9) with the help of (8). In this work a set of eight fifth order polynomial relations have been generated for  $A_p = 10^{-1}, 10^{-2}, 10^{-3}, 10^{-4}, 10^{-5}, 10^{-6}, 10^{-7}, 10^{-8}$  dB from which the first three have been shown in (8). Next we evaluate  $N$  from (10) and the truncation length  $x$  from (11) and (12). The required impulse response  $h(x)$  is then obtained from (5). Equations (7) to (12) are general and are valid any set of input specifications with the only restriction given by  $30 \leq A_s \leq 300$  dB.

The efficacy and the flexibility of this design methodology is depicted with the help of Fig. 3 to Fig. 5. Fig. 3(a) illustrates the Gaussian windowing operation represented by (5) while Fig. 3(b) shows the resultant impulse response. Comparison of magnitude response with other methods for different stopband attenuation is presented in Fig. 4. Filters designed with proposed method could achieve stopband attenuation as low as 300 dB. The maximum that we can achieve with our proposed method is about 320 dB on a 32bit Pentium IV computer. On the other hand Kaiser Window method could achieve a maximum stopband attenuation of 270 dB while the optimal method (Parks-McClellan algorithm implemented in Matlab R2006a) is unable to go beyond 200 dB. The dotted curves in Fig. 4(c) are for the failed cases with stopband attenuations 250 dB and 300 dB respectively. The high complexity of computations involved in the evaluation of the filter using optimal method, requires higher accuracy to

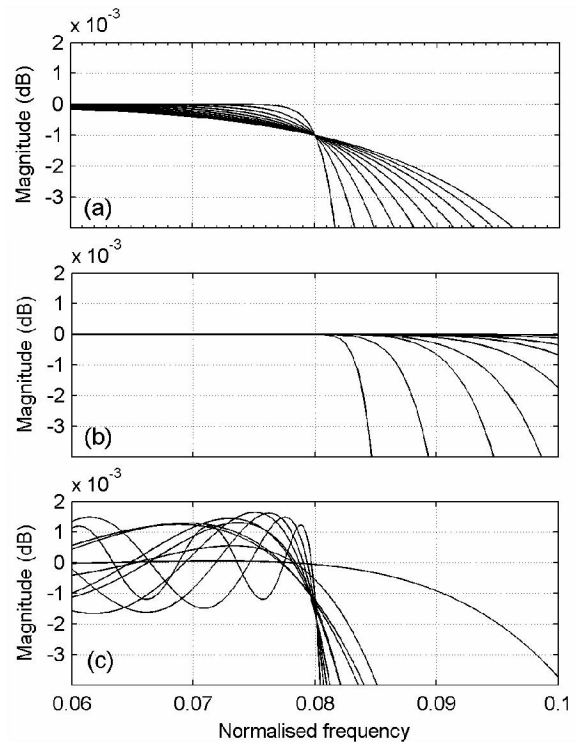


**Fig. 5.** Magnitude response curves of the filters obtained by (a) proposed method, (b) Kaiser window method and (c) optimal method (Parks-McClellan algorithm) are shown with the passband edge frequency  $f_p = 0.08$  with amplitude  $A_p = 10^{-3}$  dB and different stopband edges  $f_s = 0.12, 0.16, 0.20, 0.24, 0.28, 0.32, 0.36, 0.40, 0.44$  and  $0.48$  with amplitude  $A_s = 150$  dB. For illustration, only portions of the whole magnitude response curves are presented. The figure clearly shows all the filter curves in Fig. 5(a) pass through the designated passband edge. In comparison performance of Kaiser window is very poor while the accuracy of the optimal method is quite satisfactory.

achieve stopband attenuation beyond 200 dB and 32 bit accuracy offered by Pentium 4 machine is probably not sufficient.

In Fig. 5 comparison of the accuracy of band edge frequency control is presented. From the figure it is clear that the performance of the proposed method in Fig. 5(a) is the best. All the curves pass through the designated passband edge. Performance of the optimal method is quite satisfactory except with cases with  $f_s$  close to 0.5 while the Kaiser window performs very badly. Comparison of computational cost for various transition bands and for different methods is

TABLE I  
COMPARISON OF FILTER COMPUTATION TIME BY DIFFERENT METHODS  
 $f_p = 0.1, A_p = 10^{-3}$  dB,  $A_s = 150$  dB

$f_s / \text{time}(s)$	0.101	0.103	0.105	0.110	0.150	0.200	0.250	0.450
$t_{\text{Parks-McClellan}}$	*	3.980	1.420	0.385	0.065	0.056	0.054	0.053
$t_{\text{Kaiser}}$	0.150	0.125	0.125	0.120	0.118	0.117	0.117	0.117
$t_{\text{Gauswin}}$	0.102	0.099	0.099	0.098	0.096	0.094	0.092	0.092

\* did not converge  
\*\* time is expressed in seconds

presented in Table 1.  $t_{\text{Parks-McClellan}}$ ,  $t_{\text{Kaiser}}$  and  $t_{\text{Gauswin}}$  are computation times for the Optimal method, Kaiser window method and the proposed Gaussian window method respectively. Computation time for the optimal method (Parks-McClellan algorithm) increases sharply with the decrease in transition band width where as for Kaiser and the proposed Gaussian window method the time remains nearly the same. On an average the computation time for our proposed method is lesser though the time taken by the optimal method is the minimum only for higher transition band widths.

In all the examples the number of taps taken by our proposed method is comparable to Kaiser window method. Compared to the Optimal method the taps required for our method is on an average 1.6 times larger. It should be here noted that by increasing the number of taps does not improve the performance to be comparable to the one in Fig. 5(a). A demo of the filter is available in [8].

#### IV. CONCLUSION

We have shown that superposition of the mean shifted Gaussians can be used to construct filters. We have also derived relationships to evaluate the corresponding impulse response in a computationally efficient and non-recursive manner. We show that this method is equivalent to windowing operation by an appropriate Gaussian and demonstrate that this gives precise control over band-edge frequencies and ripple magnitude unlike conventional windowing operation. A comparison with Kaiser and optimal method (Parks-McClellan algorithm) shows that our proposed method have more precise control over band edge frequencies and is capable of designing filters with stop-band attenuation as high as 300 dB. We also show that this method is computationally efficient too. The only drawback is that the number of taps required for our method is on an average 1.6 times larger compared to that of the Optimal method. We also note that by increasing the number of taps in the Optimal method does not improve the control over band edge frequencies nor does it increase the maximum attainable stopband attenuation.

#### V. REFERENCES

- [1] A. V. Oppenheim, R. W. Schaffer and J. R. Buck, *Discrete-Time Signal Processing*. Prentice-Hall: New-Jersey, 1999, ch. 7.
- [2] E. C. Ifeachor and B. W. Jervis, *Digital Signal Processing A Practical Approach*. New Delhi: Pearson Education, 2004, ch. 7.
- [3] S. K. Mitra, *Digital Signal Processing: A Computer- Based Approach*. New Delhi: Tata McGraw-Hill, 2001, ch. 7.
- [4] L. R. Rabiner, "Techniques for designing finite-duration impulse response digital filters," *IEEE Trans. Commun. Technol.*, vol. COM-19, Apr. 1971, pp. 188–195.
- [5] S. Karmakar, K. Ghosh, S. Sarkar and S. Sen, "Design of a low-pass filter by multi-scale even order Gaussian derivatives," *Signal Processing*, vol. 86, 2006, pp. 3923-3933.
- [6] P. Kraniuskas, *Transforms in Signals and Systems*. Workingham: Addison-Wesley, 1992, ch. 2.
- [7] A. G. Tsyppkin and G. G. Tsyppkin, *Mathematical Formulas*. Moscow: Mir Publishers, 1988, ch. 4.
- [8] Digital Filter Demo,  
<http://www.saha.ac.in/med/sandip.sarkar/research.html>